

# The Effect of Human Umbilical Cord Mesenchymal Stromal Cells in Protection of Dopaminergic Neurons from Apoptosis by Reducing Oxidative Stress in the Early Stage of a 6-OHDA-Induced Parkinson's Disease Model

Cell Transplantation  
2019, Vol. 28(15) 875–995  
© The Author(s) 2019  
Article reuse guidelines:  
sagepub.com/journals-permissions  
DOI: 10.1177/0963689719891134  
journals.sagepub.com/home/cll  


Heng Chi<sup>1</sup>, Yunqian Guan<sup>1</sup>, Fengyan Li<sup>1</sup>, and Zhiguo Chen<sup>1,2,3</sup> 

## Abstract

Oxidative stress is an important cause of dopaminergic (DA) neuron apoptosis in Parkinson's disease (PD). Mesenchymal stromal cells (MSCs) possess antioxidative features. In this study, we investigated whether MSCs could reduce oxidative stress and protect DA neurons from apoptosis by intravenous (I.V.) injection in the early stage of a 6-hydroxydopamine (6-OHDA)-induced PD model. MSCs were injected into the tail vein of mice, and behavioral tests, immunofluorescence staining, western blot, and oxidative stress levels were assessed at different time points. After 6-OHDA exposure, DA neuron apoptosis was detected, together with severe oxidative stress in brain and periphery. Compared with the non-transplanted sham controls, motor function in the 6-OHDA-lesioned group after I.V. injection of MSCs was significantly improved, and the levels of DA neuron apoptosis and oxidative stress decreased. The results demonstrate that MSCs can rescue DA neurons from ongoing apoptosis by reducing oxidative stress, and provide insights on developing new therapeutic strategies to offset the degenerative process of PD.

## Keywords

human umbilical cord mesenchymal stromal cells, dopaminergic neurons, Parkinson's disease, apoptosis, oxidative stress

## Introduction

Parkinson's disease (PD) is a progressive neurodegenerative disease, and the pathogenesis is caused by degeneration of dopaminergic (DA) neurons in the substantia nigra pars compacta (SNpc), which results in decreased levels of dopamine in the striatum<sup>1</sup>. Inadequate dopamine leads to motor deficits, such as stiffness, bradykinesia, quiescent tremor, and abnormal gait. Oxidative stress has been demonstrated as one of the crucial mechanisms of DA neuron death in PD<sup>2</sup>. The neuron death pathway begins with the generation of intracellular free radicals followed by mitochondrial damage and ultimately the activation of Caspases-3/7<sup>3</sup>. According to this theory, stereotactic injection of 6-hydroxydopamine (6-OHDA) is used as a classic method for PD modeling; via the generation of reactive oxygen species (ROS), such as H<sub>2</sub>O<sub>2</sub>, 6-OHDA causes neural toxicity through intracellular enzyme oxidation and/or extracellular auto-oxidation<sup>4</sup>. In fact, H<sub>2</sub>O<sub>2</sub> acts as a second messenger by activating proteins containing oxidized thiol groups on their cysteine residues,

such as transcription factors, kinases, and oxidative sensor proteins<sup>5</sup>. Previous studies have shown that H<sub>2</sub>O<sub>2</sub> derived from 6-OHDA could trigger a series of events that lead to

<sup>1</sup> Cell Therapy Center, Beijing Institute of Geriatrics, Xuanwu Hospital Capital Medical University, National Clinical Research Center for Geriatric Diseases, and Key Laboratory of Neurodegenerative Diseases, Ministry of Education, Beijing, China

<sup>2</sup> Center of Neural Injury and Repair, Beijing Institute for Brain Disorders, Beijing, China

<sup>3</sup> Center of Parkinson's Disease, Beijing Institute for Brain Disorders, Beijing, China

Submitted: April 25, 2019. Revised: October 27, 2019. Accepted: November 6, 2019.

### Corresponding Author:

Zhiguo Chen, Cell Therapy Center, Beijing Institute of Geriatrics, Xuanwu Hospital Capital Medical University, National Clinical Research Center for Geriatric Diseases, and Key Laboratory of Neurodegenerative Diseases, Ministry of Education, 45 Changchun St, Beijing 100053, China.  
Email: chenzhiguo@gmail.com



cell death in both non-neuronal and neuronal cells<sup>6</sup>. Previous *in vitro* and *in vivo* studies have demonstrated that oxidative stress triggered by neurotoxins, such as 6-OHDA, activates the apoptotic pathway. In this mechanism, the apoptotic protein Bax is activated and results in mitochondrial outer membrane permeabilization, cytochrome c leakage, and activation of the caspase cascade<sup>7</sup>.

Currently, PD treatment is limited to pharmacological therapy, such as levodopa and monoamine oxidase B inhibitors, and surgical intervention. Although these methods are quite effective in controlling motor symptoms, side effects are evident, including motor fluctuations, such as on/off periods and dyskinesia-sudden stiffness, and involuntary movement following long-term uptake of levodopa<sup>8</sup>. Importantly, these presently available treatments cannot prevent disease progression or neurodegeneration. Mesenchymal stromal cells (MSCs) are an attractive option for cell therapy. MSCs possess immunomodulatory and neurotrophic properties. Evidence suggests that MSC-mediated protection of damaged tissue might depend on their capacity to produce factors that enhance angiogenesis, stimulate host cells to regenerate damaged tissues, and inhibit apoptosis<sup>9–12</sup>. MSCs exhibit antioxidative properties. A group of trophic factors and cytokines secreted by MSCs might have neuroprotective effects on DA neurons by reducing oxidative stress and decreasing apoptosis levels<sup>13</sup>. MSCs can be isolated from adipose tissue, bone marrow, and umbilical cord<sup>14</sup>. Among them, MSCs isolated from human umbilical cord show similar phenotypes to those derived from other tissues, and are further advantageous given that they are derived from redundant postnatal tissues and pose no ethical challenges. In addition, MSCs derived from human umbilical cord have been proposed to be not as mature as MSCs derived from other tissues<sup>15,16</sup>. Thus, our study employed MSCs isolated from Wharton's jelly of human umbilical cord.

Some studies have reported transplantation of MSCs to the striatum of a rodent PD model with intracranial surgery<sup>17,18</sup>. However, surgical transplantation is associated with issues such as direct tissue trauma, inflammation, and gliosis reaction. By contrast, intravenous (I.V.) or intra-arterial (I.A.) administration is a less invasive method that does not cause traumatic injury. Compared with I.V. delivery, I.A. delivery of cells is a more targeted means, but it may cause microvascular occlusions hindering blood flow in the brain, which is detrimental in neurodegenerative disorders, such as stroke, Alzheimer's disease, and PD<sup>19</sup>. Thus, I.V. injection is a safe alternative and has more clinical application possibilities among the transplantation routes. Moreover, I.V. injection allows cells to be distributed throughout the body, including lung, liver, and spleen. Since oxidative stress might be a systemic response, I.V. injection of MSCs may reduce oxidative stress systemically.

Most previous studies applied therapeutic interventions after the stable PD model has been established, that is, 14 days or longer after modeling, and selection of those subjects with greater than seven rotations/min<sup>20,21</sup>. At that point,

greater than 70% of DA neurons may have died. However, intervention with MSCs at an early stage has not been reported. Before the establishment of a stable PD model, the animal normally has already shown some pre-symptoms which resemble the preclinical stage of a patient with PD<sup>22</sup>. MSC infusion may likely offer a beneficial effect in those at the preclinical stage or those without obvious symptoms yet. In this study, we attempt to test whether I.V.-delivered MSCs could reduce the apoptosis level of DA neurons at the very early stage of PD and subsequently improve motor function in these mice.

## Materials and Methods

### Isolation and Culture of MSCs

Three umbilical cords were obtained from three healthy maternity donors without any medical disorders (mean age 28 years, age range 25–33) at Xuanwu Hospital Capital Medical University, Beijing, China, with the donors' written consent. The cord was rinsed with phosphate buffer saline (PBS) (Solarbio, Beijing, China), and two arteries, one vein, and the amniotic membrane were excised. Then, the jelly fraction of the cord was cut into 1–2 mm<sup>3</sup> explants and cultured in DMEM/F12 medium (Thermo, Waltham, USA) supplemented with 10% fetal bovine serum (FBS) (Thermo, Waltham, USA), 100 mg/ml penicillin/streptomycin (Solarbio, Beijing, China) in 10-cm round Petri dishes at 37°C in a humidified atmosphere of 5% CO<sub>2</sub> in air. After 3 days of culture, the remaining fragments were removed and the cells were cultured in fresh medium. The medium was changed twice a week. After 2 weeks, the tissues were discarded and the isolated growing cells (MSCs) were fed with the same medium. When the cells grew to 60% confluence, 0.25% trypsin–EDTA solution (Thermo, Waltham, USA) was used to dissociate the cells for passaging. The third passage of MSCs was used for characterization. MSCs were analyzed for the expression of CD markers by flow cytometry (Supplementary information). The properties of the cells derived from the three cords were quite equal, and the MSCs that all groups of mice in any single experiment received were from an individual umbilical cord.

### Animal Preparation and Lesion Surgery

Adult C57BL/6 mice weighing 20–25 g were used for the experiments. In total, 108 6-OHDA-lesioned mice and 24 sham operation mice were included in this study. The sample size of mice was calculated according to an online tool (<https://epitools.ausvet.io/site/samplesize>), and the mice were assigned into different groups by using a simple random sampling method<sup>23</sup>. A schematic of the experimental design is shown in Fig. 1. Mice were deeply anesthetized by intraperitoneal (i.p.) injection of 80 mg/kg ketamine (Sigma-Aldrich, Darmstadt, Germany) and 10 mg/kg xylazine (Sigma-Aldrich, Darmstadt, Germany). To ease breathing during anesthesia, each mouse received a low-dose atropine

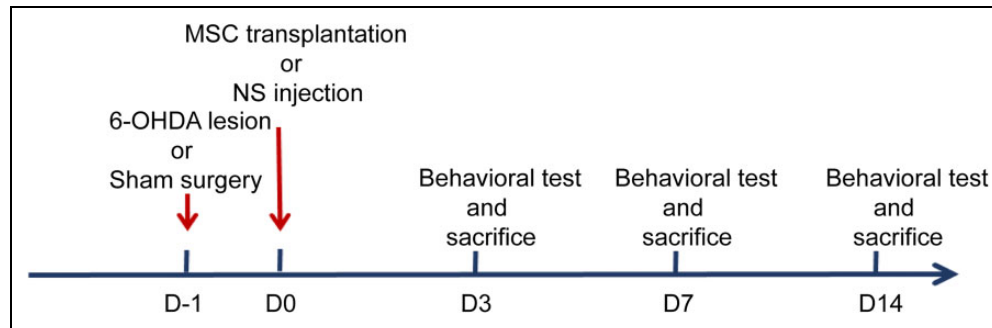


**Figure 1.** Schematic representation of experimental design. The study (132 mice in total) included the following groups: 6-OHDA MSC group ( $n = 54$ ), 6-OHDA NS group ( $n = 54$ ), Sham NS group ( $n = 18$ ), and Sham MSC group ( $n = 6$ ).

sulfate injection (0.5 mg/ml in 0.1 ml of saline). To generate a unilateral PD model, 6-OHDA (Sigma-Aldrich, Darmstadt, Germany) was injected into the striatum of the right hemisphere (A/P +0.5 mm, M/L -2.3 mm, D/V -3.2 mm). Using a stereotactic frame and microsyringe, 6-OHDA (8  $\mu$ g diluted in 0.2  $\mu$ l of 0.2% (wt/vol) ascorbic acid) was infused at a rate of 0.4  $\mu$ l/min. The microsyringes were left in the brain for an additional 5 min to allow sufficient diffusion of 6-OHDA into the brain tissue. After surgery, the animals were kept warm until they woke up. The sham group mice received the same operation except that 6-OHDA was replaced by ascorbic acid buffer only. All the mouse experiments were performed according to the guidelines for the Care and Use of Laboratory Animals established by Beijing Association for Laboratory Animal Science.

### MSC Transplantation

The second day after 6-OHDA lesioning, there was no obvious difference in symptoms across the 6-OHDA-lesioned mice. Then the 6-OHDA-lesioned mice were divided into two groups using simple random sampling method, 6-OHDA MSC group ( $n = 54$ ), and 6-OHDA NS group ( $n = 54$ ). The sham group was divided into two subgroups: Sham NS group ( $n = 18$ ), and Sham MSC group ( $n = 6$ ). On the day after surgery, MSCs were digested from the Petri dish with 0.25% trypsin. For the 6-OHDA MSC group and Sham MSC group,  $5 \times 10^5$  MSCs suspended in 200  $\mu$ l transplantation buffer (5 g/l glucose in HBSS) were injected into the tail vein of each mouse. The number of injected cells was based on previously published studies<sup>24,25</sup>. For the 6-OHDA NS group and the Sham NS group, the same volume of normal saline (NS) was injected into the tail vein. All injections were completed within 1 h.

### Behavioral Tests

The animals were tested for rotational behavior by injection of apomorphine hydrochloride (0.5 mg/kg, i.p., A4393, Sigma-Aldrich, Darmstadt, Germany) at 3, 7, and 14 days after cell injection. The basis of the rotational tests was that a denervated caudate/putamen became supersensitive to

dopamine and dopamine receptor agonists. The injured animal turned contralateral to the denervated side after administration of apomorphine, a direct dopamine receptor agonist, and the number of rotations correlated with the extent of lesion. The animals were allowed to habituate for 10 min, and then full rotations were counted in a cylindrical container (a diameter of 20 cm and a height of 30 cm) for 30 min in a quiet isolated room. The net number of rotations was defined as the positive score minus the negative score. Stable rotations ( $\geq 7$  rpm/min) were accepted as a standard for a successful PD model. 6-OHDA MSC group ( $n = 10$  on each time point), 6-OHDA NS group ( $n = 10$  on each time point), Sham NS group ( $n = 10$  on each time point), and Sham MSC group ( $n = 6$  on each time point) were included in the study.

### Immunofluorescence

After behavioral testing at different time points, mice were deeply anesthetized and perfused transcardially with PBS followed by 4% paraformaldehyde fixative. The brains and spleens were removed, postfixed in 4% paraformaldehyde for 24 h at 4°C and then cryoprotected in 30% sucrose solution. Brain and spleen sections (15  $\mu$ m thickness) were prepared, washed twice in PBS, and incubated in 0.2% Triton X-100 for 30 min at RT. Samples were blocked with 0.5% bovine serum albumin (BSA; Sigma-Aldrich, Darmstadt, Germany) for 30 min. After blocking, the sections were rinsed twice with modified PBS Tween-20 (PBST) and incubated overnight at 4°C with one or more primary antibody: rabbit anti-nuclei (Abcam, Cambridge, UK), rabbit anti-Iba1 (Abcam, Cambridge, UK), and sheep anti-TH (Sigma-Aldrich, Darmstadt, Germany). The sections were then rinsed with PBST and treated with a secondary antibody conjugated to a fluorescent dye. Secondary antibodies included donkey anti-rabbit (Jackson, West Grove, PA, USA) and donkey anti-sheep (Jackson, West Grove, PA, USA). The samples were examined using confocal microscopy. We used continuous brain sectioning, and took one out of every six slices to count the positive cells, by visual observation of the images captured by confocal microscopy.

Three slices for each mouse were counted. 6-OHDA NS group ( $n = 6$  on each time point), 6-OHDA MSC group ( $n = 6$  on each time point), Sham NS group ( $n = 6$  on D14), and Sham MSC group ( $n = 6$  on D14) were included.

### Western Blot Analysis

Protein extracts were obtained with 100  $\mu$ l of lysis buffer (150 mM NaCl, 20 mM TRIS, 1% Triton X-100, containing the Protease Inhibitor Cocktail Complete Mini, pH 8, Roche Applied Science, Basel, Switzerland). Samples (20  $\mu$ g) were separated by SDS-page on 7.5% acrylamide gel and blotted on PVDF membranes (Immobilon P; Millipore, Bedford, MA, USA) using a semidry technique. The membranes were blocked with 5% skimmed milk (Difco, Becton-Dickinson, Franklin Lakes, USA) in 0.1% Tween-20 in PBS for 2 h at room temperature. Membranes were incubated overnight at 4°C with specific primary antibodies: rabbit monoclonal anti-GAPDH (1:1000, catalog number 5174, CST, Danvers, USA), rabbit polyclonal anti-cleaved Caspase-3 (1:500, catalog number ab13847, Abcam, Cambridge, UK), rabbit polyclonal anti-Bax (1:1000, catalog number 2772s, CST, Danvers, USA), and rabbit monoclonal anti-Bcl-2 (1:2000, catalog number ab182858, Abcam, Cambridge, UK). The intensity of each band was normalized to that of GAPDH. Incubation with appropriate HRP-conjugated secondary antibody followed (goat anti-rabbit, 1:10000, Li-Cor, Lincoln, NE, USA). Immunoreactive signals were visualized using Luminoimaging Analyzer LAS-3000 (Fujifilm, Tokyo, Japan) and were analyzed by Multi Gauge software (Fujifilm, Tokyo, Japan). 6-OHDA NS group ( $n = 6$  on each time point), 6-OHDA MSC group ( $n = 6$  on each time point), and Sham NS group ( $n = 6$  on D14) were included.

### Determination of SOD, MDA, GSH, and GSH-PX Activity

Superoxide dismutase (SOD), glutathione (GSH), and glutathione peroxidase (GSH-PX) activities and malondialdehyde (MDA) levels were determined using commercially available assay kits (JianCheng, Nanjing, China). Tissues and sera were homogenized in ice-cold PBS and centrifuged, and the supernatant was obtained for SOD, MDA, GSH, and GSH-PX assay according to the manufacturer's instructions. MDA results are expressed as nmol/mg protein. GSH results are expressed as mg/g protein. GSH-PX and SOD activities are expressed as U/mg protein. 6-OHDA NS group ( $n = 6$  on each time point), 6-OHDA MSC group ( $n = 6$  on each time point), and Sham NS group ( $n = 6$  on D14) were included.

### Statistical Analysis

The experiments were performed in three independent settings. Data were expressed as the means  $\pm$  standard deviation (SD) of three independent experiments. All statistical analyses were performed using SPSS version 17.0.

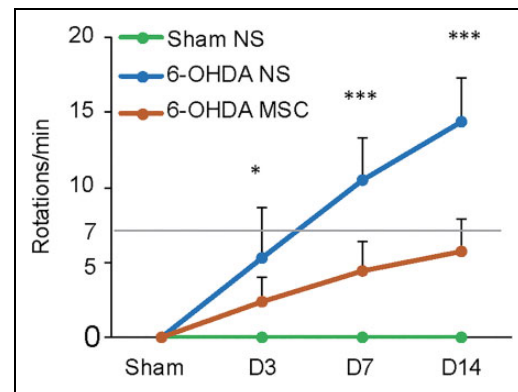


**Figure 2.** Apomorphine-induced contralateral rotations at different time points in the 6-OHDA MSC group ( $n = 10$ ), 6-OHDA NS group ( $n = 10$ ), and Sham NS group ( $n = 10$ ). Data were expressed as the mean  $\pm$  SD. \* $p < 0.05$ , \*\* $p < 0.01$ , \*\*\* $p < 0.001$ .

Differences between two groups were analyzed by independent student's *t*-test. Differences among three groups were analyzed by one-way analysis of variance (ANOVA) followed by post hoc Duncan multiple-comparisons test. We consider a value of  $p < 0.05$  as statistically significant and  $p < 0.01$  or  $p < 0.001$  as highly significant.

## Results

### Infusion of MSCs Promotes Behavioral Recovery of 6-OHDA-Lesioned Mice

MSCs were isolated from umbilical cord and cultured as a monolayer (Figure S1). Flow cytometry showed that these cells did not express markers CD11b, CD19, CD34, or CD45, but were positive for MSC markers CD73, CD90, and CD105 (Figure S1). The cells could also differentiate into adipocytes, osteoblasts, and chondrocytes (Figure S2).

Motor functions of the mice were evaluated based on apomorphine-induced rotations before cell transplantation and 3, 7, and 14 days post-transplantation. We found that throughout the 14-day time window, apomorphine caused a significant contralateral turning in the animals exposed to 6-OHDA compared with the Sham NS group (Fig. 2,  $F(1, 18) = 59.41$ ,  $p = 4.15E-07$ , at D14). Sham MSC group showed similar behavioral results as Sham NS group (data not shown). The total net number (contralateral minus ipsilateral) of rotations in the 6-OHDA MSC group on D14 was below the level of 7 rotations/min (Video S1). The total net number of rotations in the 6-OHDA NS group on D14 was above the level of 7 rotations/min (Video S2).

### Protective Effect of MSC Infusion on DA Neurons

Compared with the sham group, all animals subjected to 6-OHDA injection exhibited reduced tyrosine hydroxylase (TH) staining on the ipsilateral side of SNpc. Similarly, 6-OHDA-treated mice exhibited decreased TH expression in



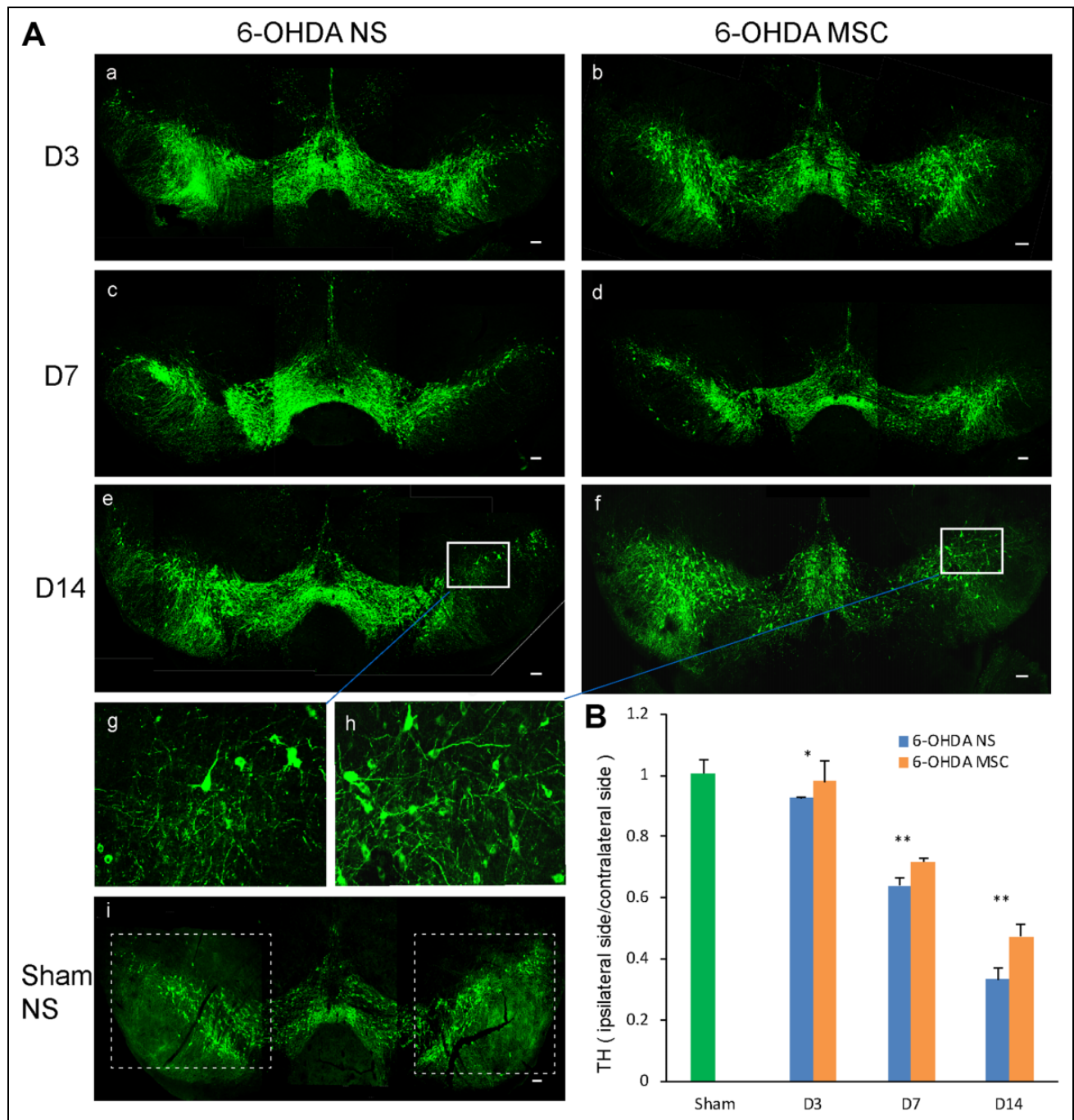


**Figure 3.** TH expression in the SNpc of mice. (A) Immunofluorescent staining for TH in the SNpc of Sham NS mice, mice exposed to 6-OHDA that received NS, and mice exposed to 6-OHDA and transplanted with MSCs at different time points. (Ag, Ah) Higher magnification of the insets in (Ae) and (Af), respectively. (B) Analysis of TH-positive cells in the SNpc. Values (mean  $\pm$  SD) represented the ratios of the number of TH<sup>+</sup> cells in the ipsilateral side to that in the contralateral side. Figures are representative of one out of three experiments. \* $p < 0.05$ , \*\* $p < 0.01$ , \*\*\* $p < 0.001$ . Scale bars: 100  $\mu$ m.

the SNpc on the side of 6-OHDA injection versus the contralateral side. Sham NS mice showed comparable levels of TH expression on both sides of SNpc (Fig. 3). Sham MSC mice also showed comparable levels of TH expression on both sides of SNpc (Figure S3). MSC infusion did not affect the motor function of Sham MSC group according to the

behavioral data. However, 6-OHDA-lesioned animals with MSC infusions showed significantly more TH-positive cells compared with the 6-OHDA NS group. MSC treatment reversed the extent of TH neuron reduction with the extension of time. Especially on D14, quantification of TH-positive cells at SNpc revealed approximately 72%

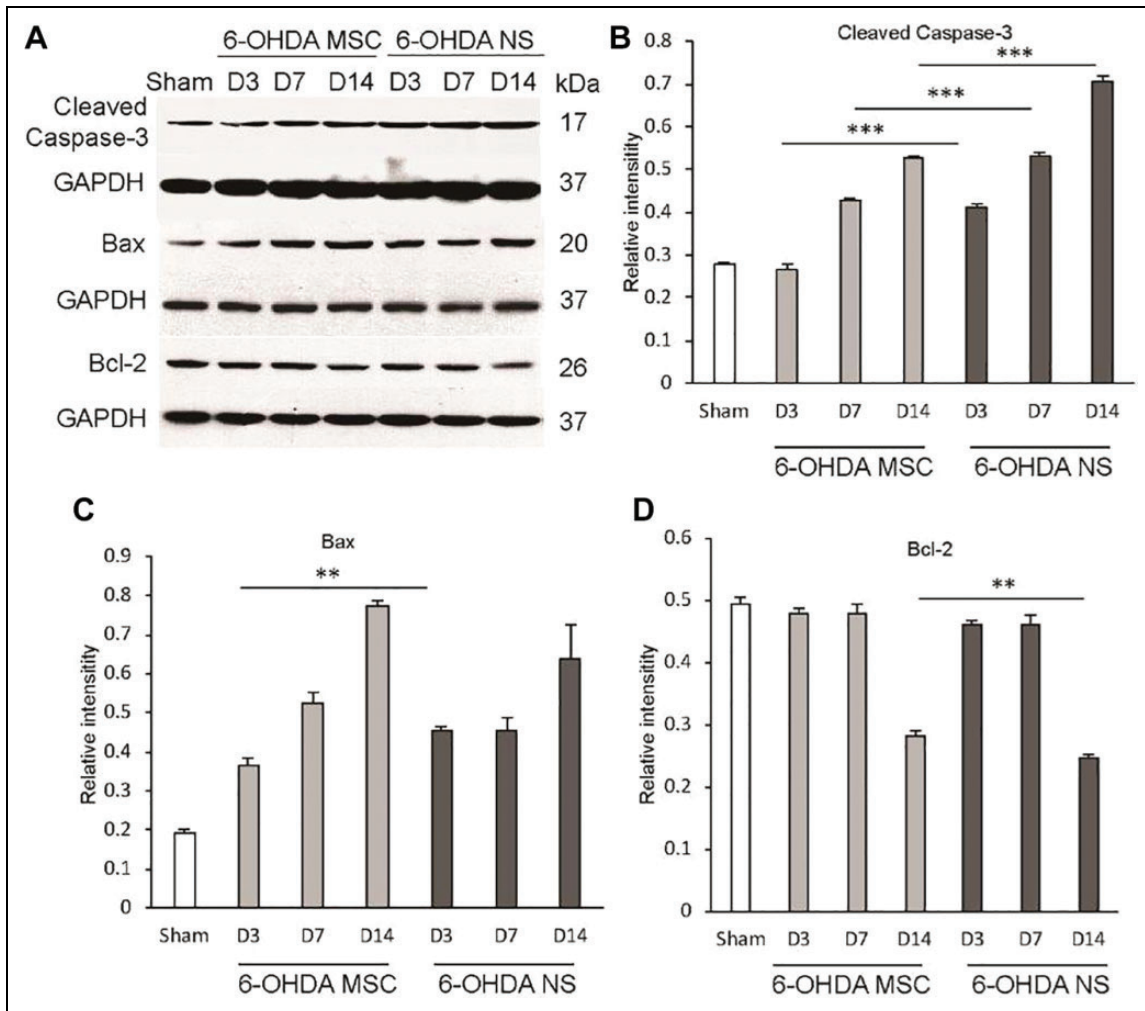


**Figure 4.** Expression levels of cleaved Caspase-3, Bax, and Bcl-2, normalized to that of GAPDH as assessed by western blotting (A-D). Data are presented as the means  $\pm$  SD ( $n = 6$  mice on each time point). Sham, Sham NS group. \* $p < 0.05$ , \*\* $p < 0.01$ , \*\*\* $p < 0.001$ .

degeneration in the 6-OHDA NS group versus approximately 53% in the 6-OHDA MSC group ( $F(1, 10) = 20.35$ ,  $p = 0.0011$  at D14). The animals showed a clear increase in the number of surviving TH-positive cell bodies and TH-positive fibers in the right side of SNpc (Fig. 3).

#### MSC Treatment Impacts 6-OHDA-Induced Activation of Proteins Related to Apoptosis

Protein was extracted from the SNpc of the 6-OHDA-lesioned hemisphere and sham operation hemisphere. The effects of MSC treatment on 6-OHDA-mediated cell death were examined by measuring the activation of Caspase-3 and the levels of the pro-apoptotic Bax protein and the anti-apoptotic Bcl-2 protein. Western blot analysis indicated that 6-OHDA injection significantly changed the levels of Bax, Bcl-2, and cleaved Caspase-3 in a time-dependent manner compared with those from the Sham NS group, and such alterations were significantly reversed by MSC treatment (Fig. 4). Compared with the 6-OHDA NS group, the levels

of cleaved Caspase-3 were reduced by approximately 26.1% (D3,  $F(1, 10) = 422.65$ ,  $p = 1.64E-09$ ), 18.9% (D7,  $F(1, 10) = 517.79$ ,  $p = 6.06E-10$ ), and 22.9% (D14,  $F(1, 10) = 1360.23$ ,  $p = 5.11E-12$ ). Bax levels were reduced by approximately 21.5% (D3,  $F(1, 10) = 20.24$ ,  $p = 0.0011$ ). Bcl-2 levels were increased by approximately 28.8% (D14,  $F(1, 10) = 12.84$ ,  $p = 0.0050$ ).

#### Distribution of Transplanted MSCs in Mice

In the brains of 6-OHDA MSC mice, including the midbrain and cortex, no I.V.-transplanted MSCs were detected at the time points examined using immunofluorescence staining for human nuclei, which is expressed by all human nucleated cells but not by murine cells. Since there were no MSCs detected in the central nervous system (CNS), we tracked the cells in the periphery. Because the spleen was the storage organ of peripheral blood, we isolated the spleens on D3, D7, and D14. The samples were sliced (at 15  $\mu$ m thickness) and stained for human nuclei. A large number of transplanted MSCs were found in the spleen and were distributed in small

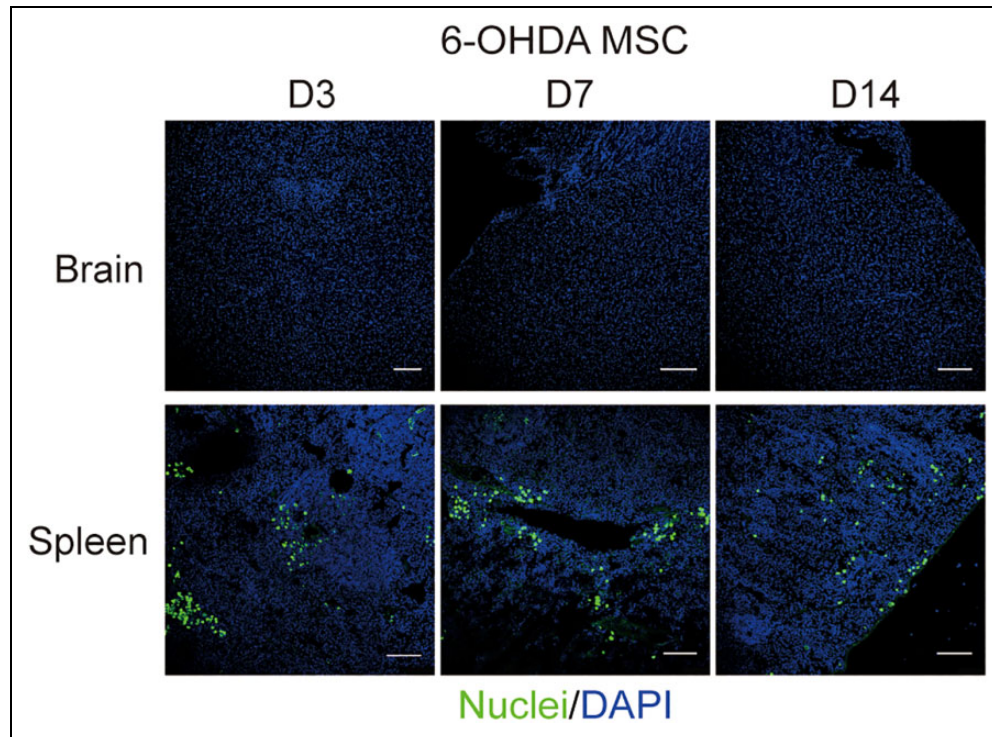


**Figure 5.** Immunofluorescent staining of brain and spleen slices for human nuclei in 6-OHDA-leisoned mice 3, 7, and 14 days after MSC transplantation. Data were expressed as the mean  $\pm$  SD. \* $p$ <0.05, \*\* $p$ <0.01, \*\*\* $p$ <0.001.

clusters. Over the 14-day time window, the number of living MSCs did not show a significant change over time in the spleen (Fig. 5).

#### **Infusion of MSCs into 6-OHDA-Treated Mice Induces Higher Expression Levels of SOD, GSH, and GSH-PX, and a Lower Level of MDA**

To determine whether the protective effects of MSCs against 6-OHDA toxicity in PD mice occurred via its antioxidant properties, we determined SOD activities and the levels of the lipid peroxidation product MDA, the deoxidizer GSH, and the antioxidative enzyme GSH-PX.

With regard to 6-OHDA-treated mice that received MSCs, SOD activity was increased by 9.0% ( $F(1, 10) = 7.66, p = 0.0199$ ), 9.8% ( $F(1, 10) = 12.23, p = 0.0058$ ), and 41.2% ( $F(1, 10) = 13.14, p = 0.0047$ ), on D3, D7, and D14, respectively, in SNpc, compared with the 6-OHDA NS group (Fig. 6). SOD activity was markedly increased by 18.9% ( $F(1, 10) = 4.88, p = 0.0516$ ), 18.7% ( $F(1, 10) = 13.94, p = 0.0039$ ), and 47.1% ( $F(1, 10) = 17.88, p = 0.0017$ ), on D3, D7, and D14, respectively, in spleen (Fig. 6). SOD activity was increased by 4.9% ( $F(1, 10) = 17.30, p = 0.0019$ ), 3.9% ( $F(1, 10) = 2.63, p = 0.1360$ ), and 17.6% ( $F(1, 10) = 8.30, p = 0.0164$ ), on D3, D7, and D14, respectively, in sera (Fig. 6).

MSC infusion resulted in a reduction in MDA levels by 22.1% ( $F(1, 10) = 3.40, p = 0.0952$ ), 24.5% ( $F(1, 10) =$

4.71,  $p = 0.0552$ ), and 47.3% ( $F(1, 10) = 8.51, p = 0.0154$ ), on D3, D7, and D14, respectively, in SNpc, compared with the 6-OHDA NS group (Fig. 6). MSC treatment led to a reduction of MDA levels by 34.1% ( $F(1, 10) = 8.03, p = 0.0177$ ), 50.1% ( $F(1, 10) = 14.98, p = 0.0031$ ), and 63.4% ( $F(1, 10) = 20.57, p = 0.0011$ ), on D3, D7, and D14, respectively, in spleen (Fig. 6). MDA levels were decreased by 33.4% ( $F(1, 10) = 4.95, p = 0.0503$ ), 33.3% ( $F(1, 10) = 20.18, p = 0.0012$ ), and 21.2% ( $F(1, 10) = 4.58, p = 0.0580$ ), on D3, D7, and D14, respectively, in sera (Fig. 6).

MSC treatment significantly enhanced GSH levels by 25.2% ( $F(1, 10) = 4.07, p = 0.0712$ , D3), 27.1% ( $F(1, 10) = 18.03, p = 0.0017$ , D7), and 146.6% ( $F(1, 10) = 69.35, p = 8.27E-06$ , D14), in SNpc, compared with the 6-OHDA NS group (Fig. 6). MSC infusion significantly enhanced GSH levels by 25.7% ( $F(1, 10) = 9.60, p = 0.0113$ , D3), 97.0% ( $F(1, 10) = 77.25, p = 5.12E-06$ , D7), and 77.5% ( $F(1, 10) = 56.29, p = 2.06E-05$ , D14), in spleen (Fig. 6). MSC infusion significantly enhanced GSH levels by 57.6% ( $F(1, 10) = 3.87, p = 0.0774$ , D3), 40.6% ( $F(1, 10) = 12.24, p = 0.0057$ , D7), and 66.9% ( $F(1, 10) = 17.06, p = 0.0020$ , D14), in sera (Fig. 6).

MSC infusion significantly enhanced expression of the antioxidant enzyme GSH-PX by 5.2% ( $F(1, 10) = 13.08, p = 0.0047$ , D3), 22.5% ( $F(1, 10) = 99.59, p = 1.62E-06$ , D7), and 47.0% ( $F(1, 10) = 56.06, p = 2.09E-05$ , D14), in SNpc, compared with the 6-OHDA NS group (Fig. 6). MSC treatment significantly upregulated GSH-PX expression by 6.4% ( $F(1, 10) = 18.24, p = 0.0016$ , D3), 14.3% ( $F(1, 10) = 80.15,$



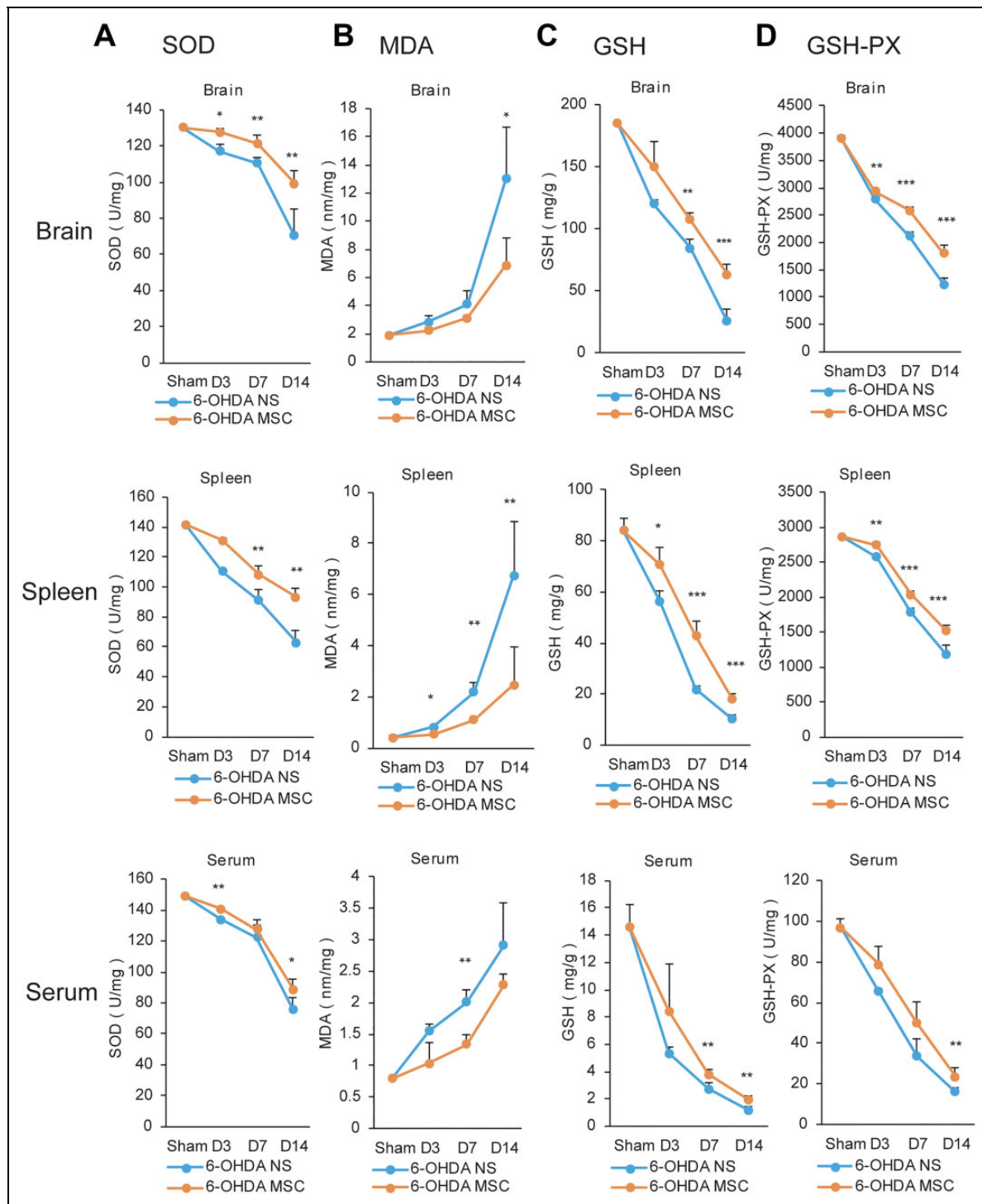


**Figure 6.** Effect of MSCs treatment on antioxidant stress in brain and periphery. (A–D) MSCs infusion upregulated the levels of SOD (A), attenuated the levels of MDA (B), and increased the levels of GSH (C) and GSH-PX (D) in the SNpc of the lesion side, spleen, and serum, of 6-OHDA-induced mice. Data were expressed as the mean  $\pm$  SD ( $n = 6$ ). Sham, Sham NS group. \* $p < 0.05$ , \*\* $p < 0.01$ , \*\*\* $p < 0.001$ .

$p = 4.34E-06$ , D7), and 28.8% ( $F(1, 10) = 39.59$ ,  $p = 9.00E-05$ , D14), in spleen (Fig. 6). MSC infusion significantly increased the level of GSH-PX by 20.1% ( $F(1, 10) = 4.69$ ,  $p = 0.0556$ , D3), 48.7% ( $F(1, 10) = 4.00$ ,  $p = 0.0734$ , D7), and 45.3% ( $F(1, 10) = 12.56$ ,  $p = 0.0053$ , D14), in sera (Fig. 6).

#### Infusion of MSCs into 6-OHDA-Treated Mice Induces Lower Expression of *Iba1*

Compared with the Sham NS group, 6-OHDA-treated mice exhibited increased *Iba1* expression at SNpc on the 6-OHDA



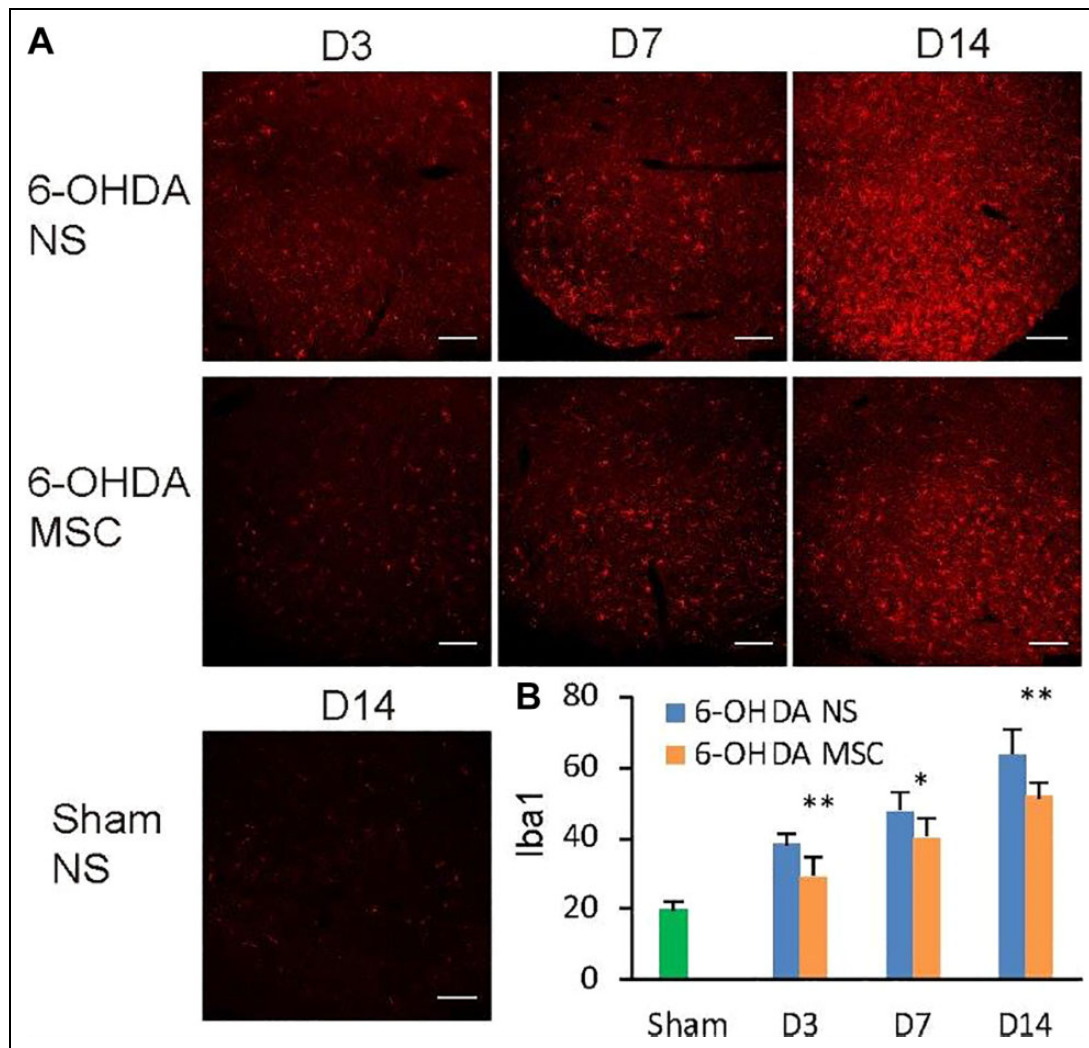


**Figure 7.** Iba1 expression on the injury side of SNpc. (A) Immunofluorescent staining for Iba1 on the injury side of SNpc from 6-OHDA NS group, 6-OHDA MSC group, and Sham NS group at different time points. (B) Analysis of the quantity of Iba1-positive cells. Data were expressed as mean  $\pm$  SD. \* $p < 0.05$ , \*\* $p < 0.01$ , \*\*\* $p < 0.001$ . Scale bars: 100  $\mu$ m.

injection side. 6-OHDA-lesioned mice with MSC infusion showed significantly fewer Iba1-positive cells compared with the 6-OHDA NS group. MSC treatment reversed upregulation of Iba1 at the different time points examined. Compared with 6-OHDA NS group, the number of Iba1-positive cells in 6-OHDA MSC group was reduced by approximately 19.1% on D14 ( $F(1, 10) = 13.70, p = 0.0041$ ) (Fig. 7).

## Discussion

The pathology showed that all animals presented with a reduction in DA neurons at SNpc after 6-OHDA was introduced (Fig. 3). The results were consistent with the behavioral data, which showed that the 6-OHDA-modeled mice rotated after induction with apomorphine and the number of rotations increased with the progression of the disease (Fig. 2). The pathogenesis of PD is considered to stimulate a series

of events leading to the activation of apoptosis responsible for irreversible DA neuronal cell death. Imbalance of the pro-apoptotic molecule Bax and the anti-apoptotic molecule Bcl-2 results in the release of cytochrome c, which subsequently activates apoptotic protease Caspase-3, which is a key executor of apoptosis<sup>26,27</sup>. Previous studies mostly examined expression of apoptotic proteins after the PD model was stabilized<sup>28,29</sup>. In our study, the acute phase was investigated, and we found that apoptosis could be detected at an early stage of 6-OHDA injury on D3 (Fig. 4). This finding indicates that DA neurons start the apoptosis process at a very early stage and might have reached a stable level after D14.

Pathological processes described in cellular and animal models have revealed that oxidative stress is a key factor involved in apoptosis<sup>30</sup>. We found that after 6-OHDA treatment, SOD, GSH, and GSH-PX activity significantly

decreased, and MDA levels increased in SNpc, spleen, and sera (Fig. 6). Substantially decreased SOD and increased MDA contents in the midbrain have been reported in 6-OHDA-lesioned rat models<sup>31,32</sup>. The MDA data in patient sera were somewhat controversial. In one study, no significant change was detected in MDA and SOD levels in PD patients' serum samples<sup>33</sup>. In contrast, another study reported a negative correlation between MDA levels in PD patient sera and severity of disease<sup>34</sup>. Wide variability was noted in the reported GSH-PX serum levels in PD, but GSH-PX levels were generally decreased<sup>35</sup>. Chen et al. have shown that oxidative damage of peripheral blood increases and the antioxidant capacity decreases in patients with PD, which is significantly correlated with disease severity<sup>36</sup>. This finding is consistent with the temporal change of oxidative stress-related molecules as observed in our study. In addition to the finding that the oxidative stress increased both in brain and peripheral blood, we found that oxidative stress was also augmented in the peripheral organs, such as spleen, which has not been reported before (Fig. 6). These results suggested that 6-OHDA-induced oxidative stress is a systemic reaction.

Neuroinflammation mediated by activated microglia has been demonstrated to contribute to PD pathogenesis. In SNpc of PD patients, abundant activated microglia were observed, which co-expressed pro-inflammatory cytokines such as TNF- $\alpha$ , IL-1 $\beta$ , and IFN- $\gamma$ , suggesting a robust inflammatory state in PD brains<sup>30,37</sup>. Evidence has emerged that chronic inflammation in PD may induce toxicity and oxidative damage in the brain. Over-activated microglia release not only cytokines, but also ROS and nitrogen groups, thus increasing the level of oxidative stress that is detrimental to DA neurons<sup>38</sup>. Studies have shown that microglia derive from monocytes or macrophages that have infiltrated into brain<sup>39,40</sup>. In addition to being of the same origin, the cellular make-ups of microglia and macrophages are very similar in terms of expressed proteins and cell surface markers. Therefore microglia and macrophages are usually considered to play similar roles in brain<sup>41,42</sup>. It was reported in adult rodent brain that a portion of Iba1<sup>+</sup> cells are derived from infiltrated monocytes/macrophages after injury, and the I.V.-injected MSCs trapped in the spleen are capable of reducing the release of monocytes/macrophages from spleen to peripheral circulation and then to brain<sup>43</sup>. The study suggests that MSCs possess a remarkable immunomodulatory property<sup>44</sup>. The immunofluorescence results in our study showed that the expression of microglia/macrophage marker Iba1 at the SNpc on the ipsilateral side was increased after 6-OHDA injection, whereas it was significantly decreased after MSC treatment. This further indicates that I.V.-infused MSCs could exert an anti-inflammatory effect in brain.

Previous studies using animal PD models have shown that I.V.-infused MSCs can cross the blood-brain barrier (BBB) and migrate into the lesion site in brain<sup>45</sup>. Another study has reported that in the 6-OHDA-induced PD model, some

I.V.-injected MSCs were detected in brain 2 days after transplantation, and cell numbers were further reduced at 1 and 4 weeks<sup>46</sup>. In fact, I.V. infusion of cells could lead to a widespread full-body distribution in peripheral organs, such as lung, liver, and spleen<sup>47</sup>. Therefore, in parallel to investigating the distribution of I.V.-injected MSCs in brain, we also examined the survival of MSCs in peripheral organs. In contrast to previous conclusions, we did not detect I.V.-transplanted MSCs in brain. In the spleen, a large number of transplanted MSCs survived for at least 14 days (Fig. 5). This finding indicates that MSCs can adapt to the peripheral environment of the host. In patients with early-stage PD, BBB permeability remains similar to age-matched controls, and BBB permeability changes were only detected in patients with advanced PD<sup>48</sup>. In our study that focused on the early stage of PD modeling, no MSCs were detected in brain. The BBB status acutely following 6-OHDA injection was not sufficient to induce MSC infiltration into the brain, or a small portion of MSCs potentially infiltrated into brain but did not survive until the time point examined.

Although the BBB may prevent cells from infiltrating into the brain, small molecules, such as free radicals, can pass through the BBB<sup>49,50</sup>. The increased free radicals in the injured brain may pass through the BBB, leading to upregulation of free radicals in the peripheral blood accordingly. Infusion of MSCs may reduce the free radicals systemically, and change the balance in brain consequently. MSCs could maintain continuous expression of SOD, catalase (CAT), and glutathione peroxidase 1 (GPX1), and a high level of glutathione that effectively removes peroxides and nitrous peroxide anions<sup>51,52</sup>. MSCs can also detoxify active substances and prevent oxidative damage to the proteome and genome<sup>53</sup>. Our finding confirmed that I.V.-infused MSCs could reduce oxidative stress in the peripheral system and the brain, where the lesions occurred (Fig. 6). Since free radicals can pass through the BBB<sup>49</sup>, after MSCs cleared harmful free radicals, such as peroxides and nitrous peroxide anions in the periphery, the free radical exchange between the peripheral region and the brain might be reduced, thus protecting the brain.

Although the I.V.-injected MSCs were not detected in the brain, the neuroprotective effect continued. The pathology showed that MSCs decreased the extent of DA neuron reduction induced by 6-OHDA. Especially on D14, quantification of DA neurons revealed approximately 72% degeneration in the 6-OHDA NS group and 53% in the 6-OHDA MSC group, representing a clear increase in both cell bodies and fibers (Fig. 3). The pathology was consistent with the behavioral test as the number of rotations correlated with the extent of lesion, showing that MSC treatment had positive effects on motor functions (Fig. 2). Western blot analysis indicated that before the PD model reached a stable state, the increasing apoptosis could be reversed by MSC treatment (Fig. 4). These results confirm the capacity of MSCs to reduce the progression of apoptosis in the early stage of PD.

The immunofluorescence staining revealed that, compared with the Sham group, the number of DA neurons on the lesion side in 6-OHDA NS group decreased by 7.95% on D3. In our study, the intervention time (D1 after 6-OHDA) was earlier than D3; therefore, it is quite likely that the neuronal loss had not reached 7.95% by D1. Patients with PD only present with clinical symptoms upon 60–80% DA neuronal loss<sup>54</sup>. Accordingly, the intervention time used in this study may correlate to a very early stage in PD development. It has been reported that exposure to certain neurotoxins, such as insecticides, herbicides, and phenothiazine antipsychotics, may cause PD<sup>55</sup>. Our study suggests that immediate treatment with MSCs might be an effective means to prevent the occurrence and progression of PD in such cases.

There are some other aspects regarding the protective mechanism of MSCs. A large body of literature has suggested that various neurotrophic factors such as vascular endothelial growth factor (VEGF), glial cell-derived neurotrophic factor (GDNF), nerve growth factor (NGF), and brain-derived neurotrophic factor (BDNF) that MSCs secrete might play a role in stimulating endogenous neurogenesis and rejuvenating damaged DA axons to reduce neuronal apoptosis<sup>56,57</sup>. And studies have shown that the levels of neurotrophic factors in the brain tissue are positively correlated with those in the serum of mice<sup>58</sup>. Other studies have shown that the exosomes secreted by MSCs carry neurotrophic factors that can reduce apoptosis<sup>59</sup>. MSC-derived exosomes contain long-chain non-coding RNA transcripts, which may increase protein kinase C expression and promote neuronal survival when neuronal damage occurs<sup>60</sup>.

## Conclusion

In summary, we showed that 6-OHDA caused high oxidative stress levels in the CNS and the peripheral system, leading DA neurons to apoptosis. I.V.-infused MSCs did not result in significant infiltration into brain but a distribution in spleen. MSC treatment had antioxidative properties and effectively protected DA neurons from apoptosis. Our findings collectively suggest the potential use of I.V. injection of MSCs for designing viable therapeutic strategies for PD treatment in the early stage of onset.

## Acknowledgments

We thank the obstetrics department of Xuanwu Hospital for providing the human umbilical cords.

## Author Contributions

Conceptualization, Z.C.; methodology, formal analysis, and investigation, H.C. Y.G, and F.L.; writing - original draft preparation, H.C.; writing - review and editing, Z.C.; supervision, Z.C.; funding acquisition, Z.C.

## Ethical Approval

Ethical approval for this study (AEEI-2015-188) was obtained from the ethics committee of Xuanwu Hospital Capital Medical University.

## Statement of Human and Animal Rights

All procedures in this study were conducted in accordance with the ethics committee of Xuanwu Hospital Capital Medical University.

## Statement of Informed Consent

Written informed consent has been obtained from healthy mothers.


## Declaration of Conflicting Interests

The author(s) declared no potential conflicts of interest with respect to the research, authorship, and/or publication of this article.

## Funding

The author(s) disclosed receipt of the following financial support for the research, authorship, and/or publication of this article: Stem Cell and Translation National Key Project (2016YFA0101403); National Natural Science Foundation of China (81973351, 81661130160, 81422014, 81561138004); Beijing Municipal Natural Science Foundation (5142005); Beijing Talents Foundation (2017000021223TD03); Support Project of High-level Teachers in Beijing Municipal Universities in the Period of 13th Five-year Plan (CIT & TCD20180333); Beijing Medical System High Level Talent Award (2015-3-063); Beijing Municipal Health Commission Fund (PXM 2018\_026283\_000002); Beijing One Hundred, Thousand, and Ten Thousand Talents Fund (2018A03); Beijing Municipal Administration of Hospitals Clinical Medicine Development of Special Funding Support (ZYLX201706); and the Royal Society-Newton Advanced Fellowship (NA150482).

## ORCID iD

Zhiguo Chen  <https://orcid.org/0000-0003-1508-510X>

## Supplemental Material

Supplemental material for this article is available online.

## References

- Ernst A, Alkass K, Bernard S, Salehpour M, Perl S, Tisdale J, Possnert G, Druid H, Frisen J. Neurogenesis in the striatum of the adult human brain. *Cell*. 2014;156(5):1072–1083.
- Dias V, Junn E, Mouradian MM. The role of oxidative stress in Parkinson's disease. *J Parkinsons Dis*. 2013;3(4):461–491.
- Hanrott K, Gudmunsen L, O'Neill MJ, Wonnacott S. 6-Hydroxydopamine-induced apoptosis is mediated via extracellular auto-oxidation and caspase 3-dependent activation of protein kinase C $\delta$ . *J Biol Chem*. 2006;281(9):5373–5382.
- Liu H, Mao P, Wang J, Wang T, Xie CH. Allicin protects PC12 cells against 6-OHDA-induced oxidative stress and mitochondrial dysfunction via regulating mitochondrial dynamics. *Cell Physiol Biochem*. 2015;36(3):966–979.
- Netto LE, Antunes F. The roles of peroxiredoxin and thioredoxin in hydrogen peroxide sensing and in signal transduction. *Mol Cells*. 2016;39(1):65–71.
- Mendivil-Perez M, Velez-Pardo C, Jimenez-Del-Rio M. Neuroprotective effect of the LRRK2 kinase inhibitor PF-06447475 in human nerve-like differentiated cells exposed to oxidative stress stimuli: implications for Parkinson's disease. *Neurochem Res*. 2016;41(10):2675–2692.

7. Perier C, Bove J, Wu DC, Dehay B, Choi DK, Jackson-Lewis V, Rathke-Hartlieb S, Bouillet P, Strasser A, Schulz JB, Przedborski S, et al. Two molecular pathways initiate mitochondria-dependent dopaminergic neurodegeneration in experimental Parkinson's disease. *Proc Natl Acad Sci U S A*. 2007; 104(19):8161–8166.
8. Morgan JC, Currie LJ, Harrison MB, Bennett JP Jr., Trugman JM, Wooten GF. Mortality in levodopa-treated Parkinson's disease. *Parkinsons Dis*. 2014;2014:426976.
9. Paul G, Anisimov SV. The secretome of mesenchymal stem cells: potential implications for neuroregeneration. *Biochimie*. 2013;95(12):2246–2256.
10. Shi Y, Su J, Roberts AI, Shou P, Rabson AB, Ren G. How mesenchymal stem cells interact with tissue immune responses. *Trends Immunol*. 2012;33(3):136–143.
11. Moloney TC, Rooney GE, Barry FP, Howard L, Dowd E. Potential of rat bone marrow-derived mesenchymal stem cells as vehicles for delivery of neurotrophins to the Parkinsonian rat brain. *Brain Res*. 2010;1359:33–43.
12. Zhenrong Z, Fangyong W, Mingjie S. The cell repair research of spinal cord injury: a review of cell transplantation to treat spinal cord injury. *J Neurorestoratology*. 2019;7:55–62.
13. Lanza C, Morando S, Voci A, Canesi L, Principato MC, Serpero LD, Mancardi G, Uccelli A, Vergani L. Neuroprotective mesenchymal stem cells are endowed with a potent antioxidant effect in vivo. *J Neurochem*. 2009;110(5):1674–1684.
14. Zhang Z, Wang X, Wang S. Isolation and characterization of mesenchymal stem cells derived from bone marrow of patients with Parkinson's disease. *In Vitro Cell Dev Biol Anim*. 2008; 44(5-6):169–177.
15. Kuh SU, Cho YE, Yoon DH, Kim KN, Ha Y. Functional recovery after human umbilical cord blood cells transplantation with brain-derived neurotrophic factor into the spinal cord injured rat. *Acta Neurochir (Wien)*. 2005;147(9):985–992; discussion 992.
16. Le Blanc K, Tammik C, Rosendahl K, Zetterberg E, Ringdén O. HLA expression and immunologic properties of differentiated and undifferentiated mesenchymal stem cells. *Exp Hematol*. 2003;31(10):890–896.
17. Delcroix GJ, Garbayo E, Sindji L, Thomas O, Vanpouille-Box C, Schiller PC, Montero-Menei CN. The therapeutic potential of human multipotent mesenchymal stromal cells combined with pharmacologically active microcarriers transplanted in hemi-parkinsonian rats. *Biomaterials*. 2011;32(6):1560–1573.
18. Danielyan L, Schäfer R, von Ameln-Mayerhofer A, Bernhard F, Verleysdonk S, Buadze M, Lourhmati A, Klopfer T, Schumann F, Schmid B, Koehle C, et al. Therapeutic efficacy of intranasally delivered mesenchymal stem cells in a rat model of Parkinson disease. *Rejuvenation Res*. 2011;14(1):3–16.
19. Ceravolo R, Volterrani D, Gambaccini G, Rossi C, Logi C, Manca G, Berti C, Mariani G, Murri L, Bonuccelli U. Dopaminergic degeneration and perfusional impairment in Lewy body dementia and Alzheimer's disease. *Neurol Sci*. 2003; 24(3):162–163.
20. Kang EJ, Lee YH, Kim MJ, Lee YM, Kumar BM, Jeon BG, Ock SA, Kim HJ, Rho GJ. Transplantation of porcine umbilical cord matrix mesenchymal stem cells in a mouse model of Parkinson's disease. *J Tissue Eng Regen Med*. 2013;7(3):169–182.
21. Khoo ML, Tao H, Meedeniya AC, Mackay-Sim A, Ma DD. Transplantation of neuronal-primed human bone marrow mesenchymal stem cells in hemiparkinsonian rodents. *PLoS One*. 2011;6(5):e19025.
22. Truong L, Allbutt H, Kassiou M, Henderson JM. Developing a preclinical model of Parkinson's disease: a study of behaviour in rats with graded 6-OHDA lesions. *Behav Brain Res*. 2006; 169(1):1–9.
23. Egbewale BE. Random allocation in controlled clinical trials: a review. *J Pharm Pharm Sci*. 2014;17(2):248–253.
24. Gutierrez-Fernandez M, Rodriguez-Frutos B, Ramos-Cejudo J, Teresa Vallejo-Cremades M, Fuentes B, Cerdan S, Diez-Tejedor E. Effects of intravenous administration of allogenic bone marrow- and adipose tissue-derived mesenchymal stem cells on functional recovery and brain repair markers in experimental ischemic stroke. *Stem Cell Res Ther*. 2013;4(1):11.
25. Park BN, Kim JH, Lee K, Park SH, An YS. Improved dopamine transporter binding activity after bone marrow mesenchymal stem cell transplantation in a rat model of Parkinson's disease: small animal positron emission tomography study with F-18 FP-CIT. *Eur Radiol*. 2015;25(5):1487–1496.
26. Li Y, Liu W, Li L, Holscher C. Neuroprotective effects of a GIP analogue in the MPTP Parkinson's disease mouse model. *Neuropharmacology*. 2016;101:255–263.
27. Desagher S, Martinou JC. Mitochondria as the central control point of apoptosis. *Trends Cell Biol*. 2000;10(9):369–377.
28. Cheng L, Chen L, Wei X, Wang Y, Ren Z, Zeng S, Zhang X, Wen H, Gao C, Liu H. NOD2 promotes dopaminergic degeneration regulated by NADPH oxidase 2 in 6-hydroxydopamine model of Parkinson's disease. *J Neuroinflammation*. 2018;15(1):243.
29. Singh S, Mishra A, Mohanbhai SJ, Tiwari V, Chaturvedi RK, Khurana S, Shukla S. Axin-2 knockdown promote mitochondrial biogenesis and dopaminergic neurogenesis by regulating Wnt/beta-catenin signaling in rat model of Parkinson's disease. *Free Radic Biol Med*. 2018;129:73–87.
30. Deleidi M, Gasser T. The role of inflammation in sporadic and familial Parkinson's disease. *Cell Mol Life Sci*. 2013;70(22): 4259–4273.
31. Wang YL, Ju B, Zhang YZ, Yin HL, Liu YJ, Wang SS, Zeng ZL, Yang XP, Wang HT, Li JF. Protective effect of curcumin against oxidative stress-induced injury in rats with Parkinson's disease through the Wnt/ beta-catenin signaling pathway. *Cell Physiol Biochem*. 2017;43(6):2226–2241.
32. Baillet A, Chantepedrix V, Trocme C, Casez P, Garrel C, Besson G. The role of oxidative stress in amyotrophic lateral sclerosis and Parkinson's disease. *Neurochem Res*. 2010; 35(10):1530–1537.
33. Gokce Cokal B, Yurtdas M, Keskin Guler S, Gunes HN, Atac Ucar C, Aytac B, Durak ZE, Yoldas TK, Durak I, Cubukcu HC. Serum glutathione peroxidase, xanthine oxidase, and superoxide dismutase activities and malondialdehyde levels in patients with Parkinson's disease. *Neurol Sci*. 2017;38(3):425–431.
34. Sanyal J, Bandyopadhyay SK, Banerjee TK, Mukherjee SC, Chakraborty DP, Ray BC, Rao VR. Plasma levels of lipid



- peroxides in patients with Parkinson's disease. *Eur Rev Med Pharmacol Sci.* 2009;13(2):129–132.
35. Abraham S, Soundararajan CC, Vivekanandhan S, Behari M. Erythrocyte antioxidant enzymes in Parkinson's disease. *Indian J Med Res.* 2005;121(2):111–115.
  36. Chen CM, Liu JL, Wu YR, Chen YC, Cheng HS, Cheng ML, Chiu DT. Increased oxidative damage in peripheral blood correlates with severity of Parkinson's disease. *Neurobiol Dis.* 2009;33(3):429–435.
  37. Sekiyama K, Sugama S, Fujita M, Sekigawa A, Takamatsu Y, Waragai M, Takenouchi T, Hashimoto M. Neuroinflammation in Parkinson's disease and related disorders: a lesson from genetically manipulated mouse models of alpha-synucleinopathies. *Parkinsons Dis.* 2012;2012:271732.
  38. Dutta SK, Verma S, Jain V, Surapaneni BK, Vinayek R, Phillips L, Nair PP. Parkinson's disease: the emerging role of gut dysbiosis, antibiotics, probiotics, and fecal microbiota transplantation. *J Neurogastroenterol Motil.* 2019;25(3):363–376.
  39. Ginhoux F, Lim S, Hoeffel G, Low D, Huber T. Origin and differentiation of microglia. *Front Cell Neurosci.* 2013;7:45.
  40. Moehle MS, West AB. M1 and M2 immune activation in Parkinson's disease: foe and ally? *Neuroscience.* 2015;302:59–73.
  41. Butovsky O, Jedrychowski MP, Moore CS, Cialic R, Lanser AJ, Gabrieli G, Koeglsperger T, Dake B, Wu PM, Doykan CE, Fanek Z, et al. Identification of a unique TGF-beta-dependent molecular and functional signature in microglia. *Nat Neurosci.* 2014;17(1):131–143.
  42. Gautier EL, Shay T, Miller J, Greter M, Jakubzick C, Ivanov S, Helft J, Chow A, Elpek KG, Gordonov S, Mazloom AR, et al; Immunological Genome Consortium. Gene-expression profiles and transcriptional regulatory pathways that underlie the identity and diversity of mouse tissue macrophages. *Nat Immunol.* 2012;13(11):1118–1128.
  43. Guan Y, Li X, Yu W, Liang Z, Huang M, Zhao R, Zhao C, Liu Y, Zou H, Hao Y, Chen Z. Intravenous transplantation of mesenchymal stem cells reduces the number of infiltrated Ly6C(+) cells but enhances the proportions positive for BDNF, TNF-1alpha, and IL-1beta in the infarct cortices of dMCAO Rats. *Stem Cells Int.* 2018;2018:9207678.
  44. Cheng Z, He X. Anti-inflammatory effect of stem cells against spinal cord injury via regulating macrophage polarization. *J Neurorestoratology.* 2017;5:31–38.
  45. Ren C, Guingab-Cagmat J, Kobeissy F, Zoltewicz S, Mondello S, Gao M, Hafeez A, Li N, Geng X, Larner SF, Anagli J, et al. A neuroproteomic and systems biology analysis of rat brain post intracerebral hemorrhagic stroke. *Brain Res Bull.* 2014;102:46–56.
  46. Wang F, Yasuhara T, Shingo T, Kameda M, Tajiri N, Yuan WJ, Kondo A, Kadota T, Baba T, Tayra JT, Kikuchi Y, et al. Intravenous administration of mesenchymal stem cells exerts therapeutic effects on parkinsonian model of rats: focusing on neuroprotective effects of stromal cell-derived factor-1alpha. *BMC Neurosci.* 2010;11:52.
  47. Hauger O, Frost EE, van Heeswijk R, Deminiere C, Xue R, Delmas Y, Combe C, Moonen CT, Grenier N, Bulte JW. MR evaluation of the glomerular homing of magnetically labeled mesenchymal stem cells in a rat model of nephropathy. *Radiology.* 2006;238(1):200–210.
  48. Pisani V, Stefani A, Pierantozzi M, Natoli S, Stanzione P, Franciotta D, Pisani A. Increased blood-cerebrospinal fluid transfer of albumin in advanced Parkinson's disease. *J Neuroinflammation.* 2012;9:188.
  49. Micheal P, PA R. Blood-brain barrier: a definition of normal and altered function. *Neurosurgery.* 1980;6(6):675–685.
  50. Karamanos Y, Gosselet F, Dehouck MP, Cecchelli R. Blood-brain barrier proteomics: towards the understanding of neurodegenerative diseases. *Arch Med Res.* 2014;45(8):730–737.
  51. Valle-Prieto A, Conget PA. Human mesenchymal stem cells efficiently manage oxidative stress. *Stem Cells Dev.* 2010;19(12):1885–1893.
  52. Dey R, Kemp K, Gray E, Rice C, Scolding N, Wilkins A. Human mesenchymal stem cells increase anti-oxidant defences in cells derived from patients with Friedreich's ataxia. *Cerebellum.* 2012;11(4):861–871.
  53. Salmon AB, Perez VI, Bokov A, Jernigan A, Kim G, Zhao H, Levine RL, Richardson A. Lack of methionine sulfoxide reductase A in mice increases sensitivity to oxidative stress but does not diminish life span. *FASEB J.* 2009;23(10):3601–3608.
  54. Greffard S, Verny M, Bonnet A, Beinis J, Gallinari C, Meaume S, Piette F, Hauw J, Duyckaerts C. Motor score of the Unified Parkinson disease rating scale as a good predictor of Lewy body-associated neuronal loss in the substantia nigra. *Arch Neurol.* 2006;63(4):584–588.
  55. Fleming SM. Mechanisms of gene-environment interactions in Parkinson's disease. *Curr Environ Health Rep.* 2017;4(2):192–199.
  56. Yan M, Sun M, Zhou Y, Wang W, He Z, Tang D, Lu S, Wang X, Li S, Wang W, Li H. Conversion of human umbilical cord mesenchymal stem cells in Wharton's jelly to dopamine neurons mediated by the Lmx1a and neurturin in vitro: potential therapeutic application for Parkinson's disease in a rhesus monkey model. *PLoS One.* 2013;8(5): e64000.
  57. Li JF, Yin HL, Shuboy A, Duan HF, Lou JY, Li J, Wang HW, Wang YL. Differentiation of hUC-MSC into dopaminergic-like cells after transduction with hepatocyte growth factor. *Mol Cell Biochem.* 2013;381(1–2):183–190.
  58. Lang UE, Hellweg R, Gallinat J. BDNF serum concentrations in healthy volunteers are associated with depression-related personality traits. *Neuropsychopharmacology.* 2004;29(4):795–798.
  59. Koniusz S, Andrzejewska A, Muraca M, Srivastava AK, Janowski M, Lukomska B. Extracellular vesicles in physiology, pathology, and therapy of the immune and central nervous system, with focus on extracellular vesicles derived from mesenchymal stem cells as therapeutic tools. *Front Cell Neurosci.* 2016;10:109.
  60. El Bassit G, Patel RS, Carter G, Shibu V, Patel AA, Song S, Murr M, Cooper DR, Bickford PC, Patel NA. MALAT1 in human adipose stem cells modulates survival and alternative splicing of PKCdeltaII in HT22 cells. *Endocrinology.* 2017;158(1):183–195.